Journal of Applied Mechanics and Technical Physics, Vol. 46, No. 4, pp. 489–495, 2005

INTERACTION OF INTERNAL GRAVITY CURRENT WITH AN OBSTACLE ON THE CHANNEL BOTTOM

E. V. Ermanyuk and N. V. Gavrilov

UDC 532.59

The problem of hydrodynamic loads arising from the interaction of gravity currents with an obstacle on the channel bottom was studied experimentally. The gravity-current structure was visualized at the stage of formation and at the stage of interaction with the obstacle. The dependence of the propagation velocity of the gravity-current front on the nondimensional current depth and the Archimedes number was studied. In the region of self-similarity in the Archimedes number, the behavior of hydrodynamic-load coefficients was studied as a function of the nondimensional gravity current depth.

Key words: *stratified fluid, gravity current, hydrodynamic load.*

Introduction. The problems of estimating the propagation velocity of gravity currents and the hydrodynamic loads induced by these currents on various obstacles are of great practical importance. In particular, much attention has been given to the dynamics of snow avalanches (see a review [1]). In oceans, an analog of such currents are gravity turbidity currents that propagate down seamounts covered with bottom sediments (see a review [2]). Such currents are a great hazard to underwater vehicles and service lines. In the present work, we studied experimentally the model problem of the action of internal gravity current due to intrusion of a denser fluid into fresh water on an obstacle on the channel bottom. The subrange of the problem parameters is determined in which the fluid viscosity effects are self-similar (in particular, the propagation velocity of the current front does not depend on the particular value of the Archimedes number), because of which the main modeling criterion is the Froude number. For this subrange of the parameters, the characteristic values of the hydrodynamic loads generated by gravity currents at submerged obstacles are determined as functions of the ratio of the vertical dimension of the current core to the total fluid depth.

Experimental Technique. A diagram of the experimental setup is shown in Fig. 1. The experiments were performed in a $320 \times 20 \times 12$ cm hydrodynamic tank separated by a partition 1 into two equal parts. The left half of the tank was filled with pure water of density ρ_1 and depth H, and the right half with an aqueous solution of sugar of density ρ_2 and depth h_2, above which there was a pure water layer of density ρ_1 and depth h_1; $h_1 + h_2 = H$. In the experiments, the depth ratio h_2/H was varied in the range $0.1 < h_2/H < 0.84$. To analyze the role of the scale effect, we performed experimental measurements of the gravity current characteristics at $H = 6$ cm and $H = 10$ cm. When the partition was removed, an internal gravity current 2 propagated to the left over the tank bottom and a depression wave 3 (the dashed curves in Fig. 1) propagated in the right part of the tank.

The instantaneous hydrodynamic loads resulting from the interaction of gravity currents with an obstacle in the shape of a rectangular cylinder 4 of height $b = 2$ cm and width 1 cm were measured using a two-component hydrodynamic balance 5 [3]. The gap between the lower surface of the rectangular-cylinder cross section and the tank bottom was 0.5 mm. The analog signal from the hydrodynamic-load sensors and wavemeter 6 was processed on a computer furnished with a 12-digit analog-to-digital converter. The gravity-current pattern and its interaction with the submerged obstacle were recorded with a digital camera. Visualization was performed using the following technique [3, 4]: a luminous screen with a grid of inclined lines drawn on it was photographed through the water

Lavrent'ev Institute of Hydrodynamics, Siberian Division, Russian Academy of Sciences, Novosibirsk 630090; ermanyuk@hydro.nsc.ru. Translated from Prikladnaya Mekhanika i Tekhnicheskaya Fizika, Vol. 46, No. 4, pp. 39–46, July–August, 2005. Original article submitted October 13, 2004.

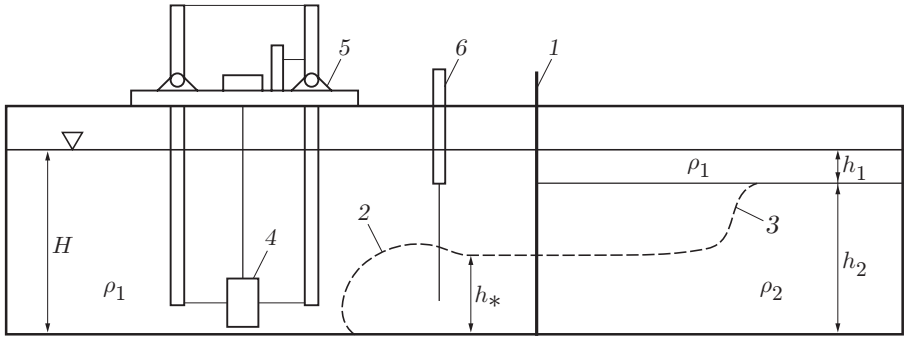

Fig. 1. Diagram of the experimental setup.

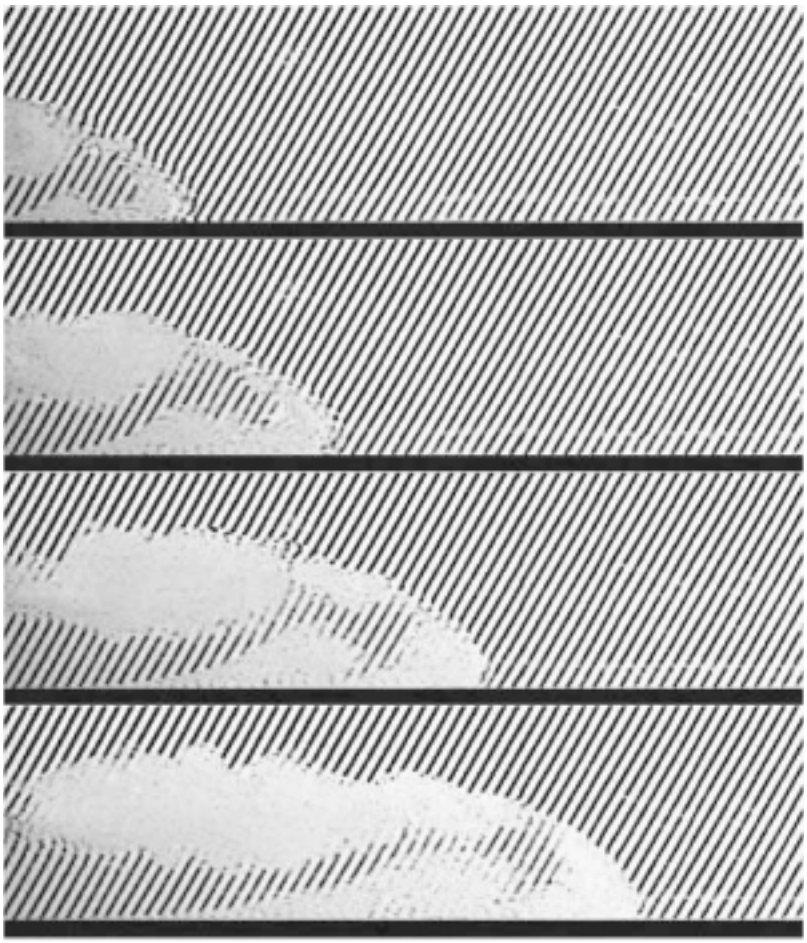

Fig. 2. Development of the mixing process at the current head for $\alpha = 0.4$, $H = 10$ cm, and $\varepsilon = 0.01$: the interval between the frames is $\Delta t = 1.27$ sec; the left boundary of the frame is at a distance $L/H = 0.5$ from the partition; the horizontal dimension of the frame is $2H$.

layer. In zones with a high density gradient, a characteristic distortion of these lines was observed, and in active-mixing zones there was a loss of the optical transparency of the fluid.

Experimental Results. In the present study, experimental information on the structure of developed gravity currents [3] is supplemented by a detailed visualization of the initial stage of current formation. The structure of the current that arises after the removal of the partition is shown in Fig. 2. Shear instability on the boundary between the upper and lower layers gives rise to regions of intense mixing, which increase with time. Near the bottom there is also a region of intense mixing. At the gravity-current head, the region occupied by a nonmixed

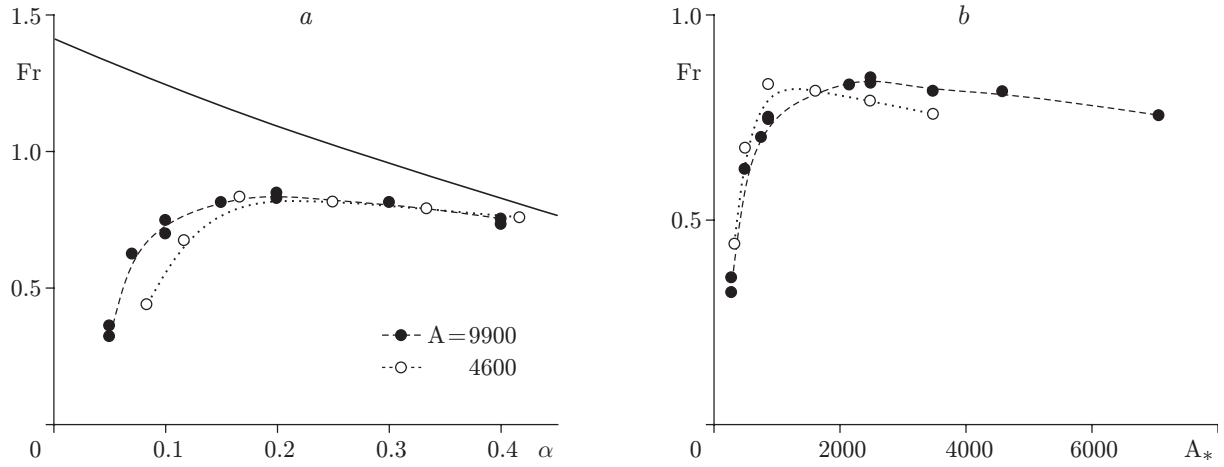

Fig. 3. Froude number versus nondimensional current depth α (a) and local Archimedes number $A_* = A(2\alpha)^{3/2}$ (b) for various values of the criterion A.

fluid of density ρ_2 decreases with time. In the fully developed gravity current, the entire current head is a visually opaque region of mixed fluid. The energy loss in mixing and overcoming the friction against the tank bottom leads to a decrease in the propagation velocity of the current front V compared to its value predicted by the ideal fluid model [5]. For the Froude number defined as $\mathrm{Fr} = V/\sqrt{\varepsilon g h_*}$ [$\varepsilon = (\rho_2 - \rho_1)/\rho_1$, g is the acceleration of gravity, and h_* is the gravity-current depth behind the head], the model of [5] gives the estimate

$$\mathrm{Fr}\,(\alpha) = \Big(\frac{(1-\alpha)(2-\alpha)}{1+\alpha}\Big)^{1/2}, \tag{1}$$

where $\alpha = h_*/H$. In practice, the parameter h_* is usually assumed to be the depth of the nonmixed current core [2]. A visual observation of the current pattern in the present problem showed that it is possible to set $h_* = h_2/2$. Below, as the parameter α we use the quantity $\alpha = h_2/(2H)$. In a system of two miscible fluids, the gravity-current velocity is determined by the following basic dimensional parameters: ρ_1, ρ_2, g, h, H, ν_1, ν_2, and æ (ν_1 and ν_2 are the kinematic viscosities of the fluids of density ρ_1 and ρ_2, respectively, and æ is the diffusion coefficient of the substance that produces stratification). In our experiments, the relative difference of the fluid densities ε was small, the physical properties of the fluid of density ρ_1 did not change, and the Schmidt number $\mathrm{Sc} = \nu_2/æ$ was large (about 10^3), so that its variation did not influence the results of the experiments. Therefore, the experimental results are conveniently represented in nondimensional form as a family of curves of $\mathrm{Fr}(\alpha)$ obtained for various values of the Archimedes number $\mathrm{A} = (\varepsilon g H^3/\nu_2^2)^{1/2}$, which characterizes the maximum (at $h_2 = H$) ratio of the buoyancy to viscosity forces. In this case, the use of the Archimedes number, which is determined by the initial parameters of the problem (i.e., which is a similarity parameter) is preferred over the traditionally used Reynolds number $\mathrm{Re} = V h_*/\nu_2$ [2], which includes the *a priori* unknown parameters V and h_*. A similar situation arises in the problem of free motion of a body in a fluid under gravity [6, 7].

Generally speaking, the propagation velocity of gravity currents depends on the distance L traveled by the current front from the partition 1. However, in the so-called inertial mode, the velocity of the front depends weakly on L [2]. For definiteness, in the present work the velocity V was measured at $L/H = 4$ from the partition. At such a distance, the structure of the current head can be considered to be completely formed [8]. Experimental curves of $\mathrm{Fr}(\alpha)$ obtained for various different values of A are presented in Fig. 3a, where the solid curve refers to the theoretical curve (1). It is evident that the experimental points are below the theoretical curve. Assuming that after the removal of the partition, the perturbation fronts move to the right and left at the same velocity and that $h_* = h_2/2$, from the conservation law of mechanical energy we obtain the estimate $\mathrm{Fr}(\alpha) = (1-\alpha)^{1/2}$. This estimate is in good agreement with experimental data. A detailed discussion of the various approaches to estimating the propagation velocity of gravity currents is given in [9]. For small α, the value of the Froude number decreases sharply because of an increase in the viscous loss due to friction against the bottom in the thin lower layer of the fluid, for which it is possible to introduce the local Archimedes number $\mathrm{A}_* = (\varepsilon g h_2^3/\nu_2^2)^{1/2} = (2\alpha)^{3/2}\,\mathrm{A}$.

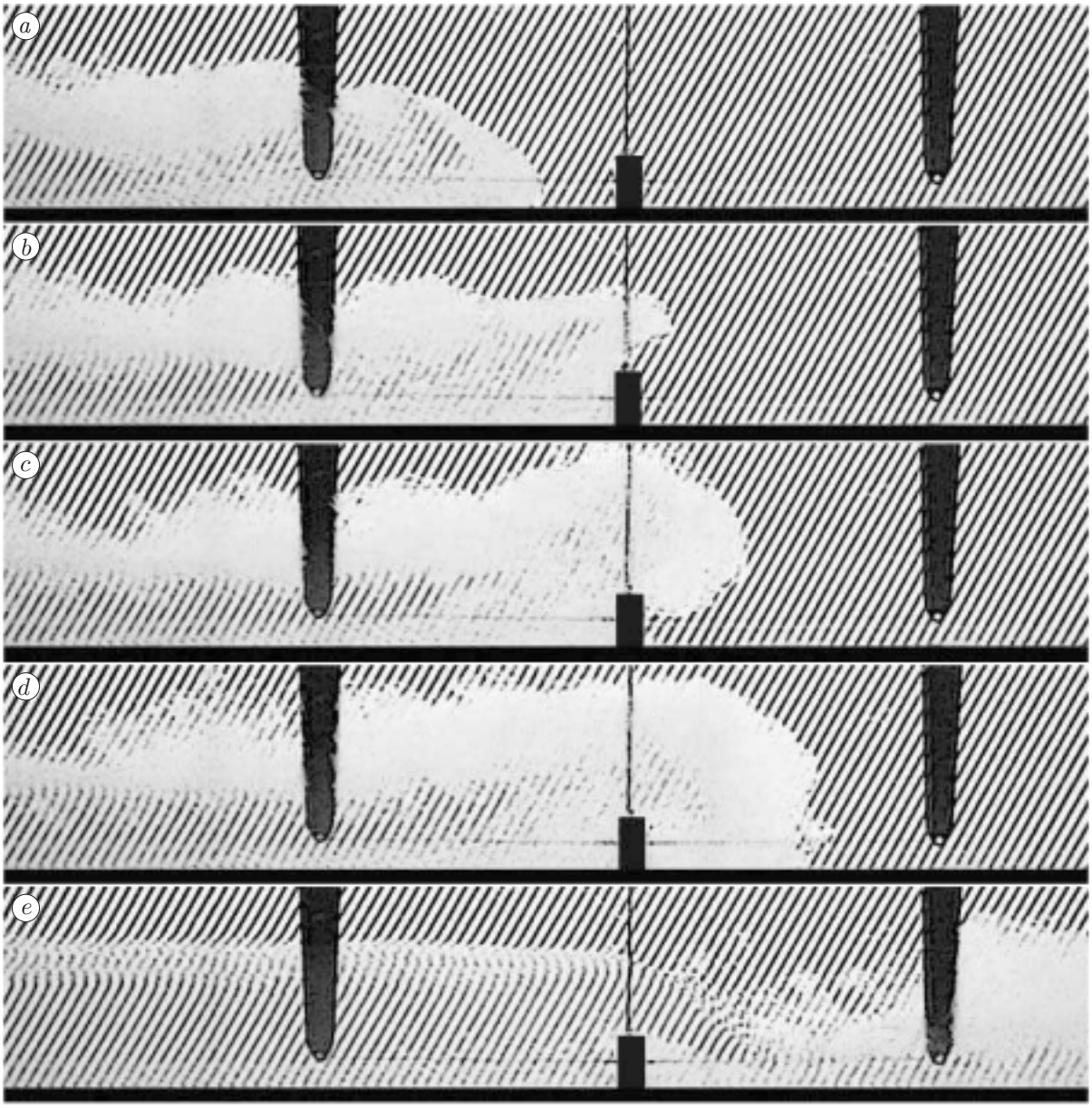

Fig. 4. Gravity current flow an obstacle for $\varepsilon = 0.01$, $H = 10$ cm, and $\alpha = 0.4$: the time step between frames a–d is $\Delta t = 1.27$ sec, and that between frames d–e is $\Delta t = 7.6$ sec.

Figure 3b gives experimental curves of the Froude number versus the local Archimedes number A_*. It is evident that the data obtained for various values of A have a common asymptotic behavior for small A_* (of order $A_* < 500$). Thus, for rather small α in experiments, the dynamic characteristics of the current in the thin fluid layer at the bottom cease to depend on α and are functions of the local Archimedes number A_*. An increase in the global Archimedes number leads to an increase in the range of α in which the experimental data for the dependence $\mathrm{Fr}(\alpha)$ have a universal nature (see Fig. 3a). According to the data presented in Fig. 3, one might expect that in the experiments performed for A = 9900 and $\alpha \geqslant 0.15$, the results of measurement of the dynamic effect of the gravity current on the bottom at the tank are self-similar for large A. Thus, as is shown in the experiments of [3], Froude modeling is performed. The data presented in Fig. 3 suggest that in experimental studies of discontinuity decay under conditions of self-similarity in A, it is at least necessary to require that $A_* > 1600$.

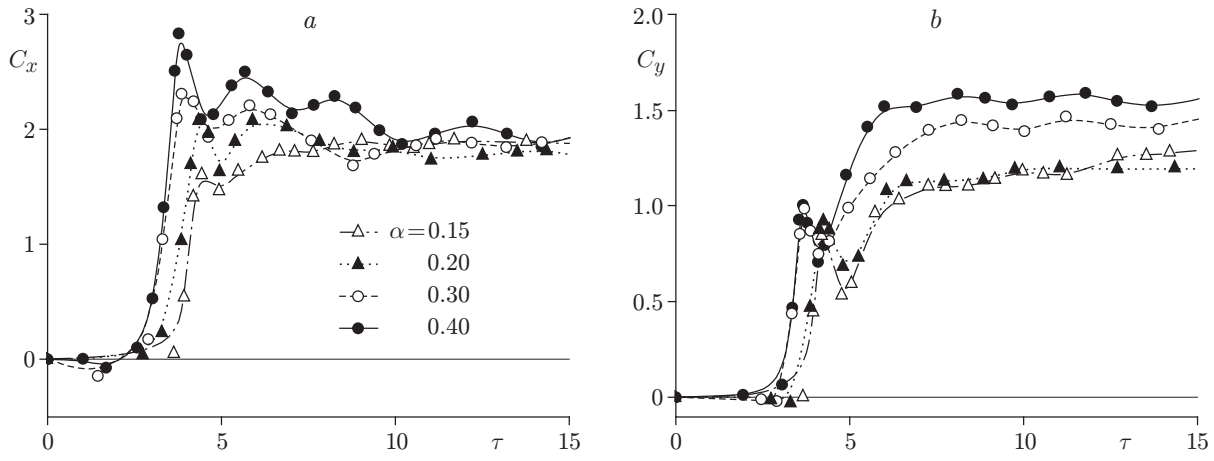

Fig. 5. Horizontal (a) and vertical (b) hydrodynamic-load coefficients versus nondimensional time τ for various nondimensional gravity-current depths α.

We also note that the obstacle used in the experiments has a rectangular cross section. It is known that because of separations at the sharp edges, a self-similar regime of current flow over such obstacles is reached at moderate Reynolds numbers (see, for example, [10]). The current pattern near the obstacle is shown in Fig. 4. The impact of the current head on the obstacle leads to current separation, accompanied by formation of a jet flow (Fig. 4b). At the successive times, undular bore type flow is produced ahead of the obstacle, and a hydraulic jump is formed behind the obstacle (Fig. 4e).

The curves of the hydrodynamic-load coefficients versus time presented in Fig. 5 are obtained for $\varepsilon = 0.02$, $H = 10$ cm, and A = 9900. The abscissa plots the nondimensional time $\tau = Vt/H$ reckoned from the time the current front passes the wavemeter 6 (see Fig. 1), and the ordinate plots the horizontal C_x (Fig. 5a) and vertical C_y (Fig. 5b) load coefficients defined as $C_{x,y} = 2F_{x,y}/(\rho_2 V^2 b)$ ($F_{x,y}$ are the loads per unit length of the obstacle). After a time period $\Delta\tau \approx 10$ from the beginning of interaction of the body with the current front, a quasistationary current regime is established and the values of the horizontal load coefficients C_x obtained for various α are close ($C_x \approx 2$).

For $\alpha = 0.4$, i.e., for the maximum value of this parameter in the present experiments, the peak horizontal load developed during the interaction with the current head exceeds the quasistationary load by a factor of 1.5. A decrease in α leads to a reduction in the ratio of the peak horizontal load to its quasistationary value. The attenuation of the undulations of C_x due to a decrease in α can be explained qualitatively by the fact that, according to (1), the values of Fr increase with decrease in α. It is known that an increase in the Froude number in flows over obstacles weakens the trend toward the formation of upstream undular bores and enhances the trend toward the formation of bore type currents with a breaking leading front [11].

In contrast to the horizontal load, the vertical-load coefficients C_y obtained at the moment of interaction of the current head with the obstacle are smaller than the quasistationary values for large times τ. As is evident from Fig. 5b, a jet flow with a separation at the corner point of the body is formed at the moment of impact. Accordingly, the current velocity directly above the body and the suction force acting on the top of the obstacle are small. Apparently, the local maximum of the vertical load under the impact is related to a pressure rise in the gap between the lower surface of the obstacle and the tank bottom. At large times, flow over the obstacle forms and a suction force of considerable magnitude arises.

The effect of flow blocking by the obstacle becomes apparent if the data are represented in a different normalization. It is known [12], that the stationary incidence of a flat horizontal jet of an ideal fluid on a vertical wall gives rise to the dynamic load $\rho V_0^2 h_0$ (ρ is the density, V_0 is the velocity, and h_0 is the jet thickness), which is equal to the total dynamic-momentum flux of the jet. In the experiments described here, the total dynamic-momentum flux of the jet of the lower fluid layer is characterized by the quantity $\rho_2 V^2 h_2/2$. Accordingly, it is possible to introduce the nondimensional coefficients $C^*_{x,y} = 2F_{x,y}/(\rho_2 V^2 h_2)$, which are linked to the previously introduced coefficients by the relation $C^*_{x,y} = C_{x,y} H/(b\alpha)$. Curves of $C^*_x(\tau)$ and $C^*_y(\tau)$ obtained for various values

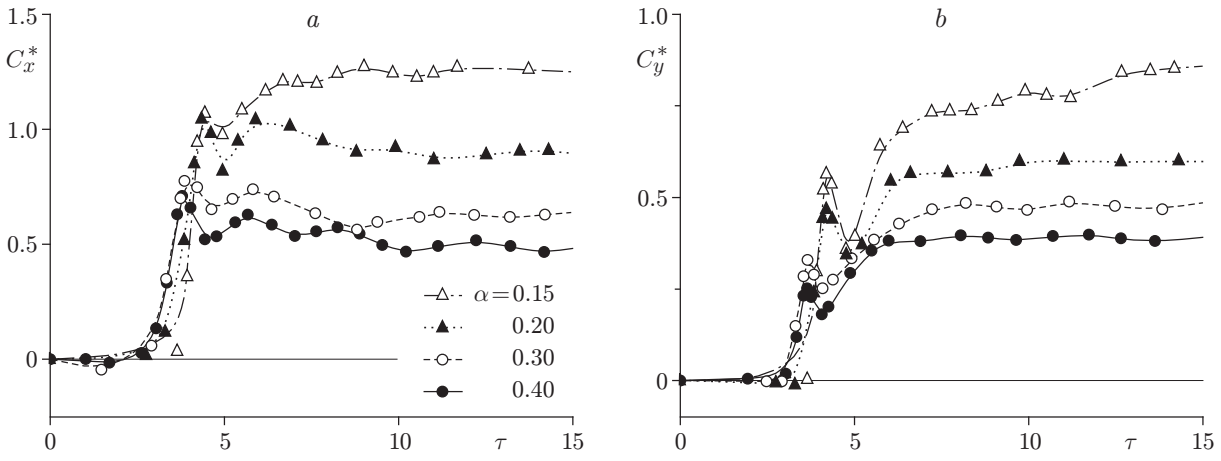

Fig. 6. Flow blocking effect for dependences $C_x^*(\tau)$ and $C_y^*(\tau)$ for various values of α.

of α are given in Fig. 6. As one might expect, for an obstacle of unchanged height b, the characteristic values of $C_x^*(\tau)$ increase with decrease in α because in this case the ratio b/h_2 increases and the effect of flow blocking by the obstacle becomes greater. A similar effect occurs for curves of $C_y^*(\tau)$ obtained for various α. In [13], the ratio of the fluid flow over an obstacle to the fluid flow in the gravity current upstream of the obstacle is considered as a parameter that characterizes the blocking effect. In our work, this information is supplemented by experimental studies of the hydrodynamic loads that characterize the momentum flux in the system. The above-stated features in the behavior of hydrodynamic loads can serve to refine estimates of the dynamic effect exerted on obstacles by powder avalanches [1], which behave as a Newtonian fluid.

Conclusions. The present study showed that in the problem of discontinuity decay in a system of two miscible fluids, experimental data on the propagation velocities of gravity current fronts are conveniently represented as a dependence of the characteristic Froude number on two parameters: α (the ratio of the gravity current depth to the total fluid depth) and A (the Archimedes number determined from the total fluid depth). For measurements under conditions of self-similarity in A, the local Archimedes number A_* (determined from the depth of the lower fluid layer) should exceed 1600. Measurements were performed of the hydrodynamic loads induced by a gravity current over an obstacle on the tank bottom. It was shown that at the stage of interaction of the body with the current head, the nonstationary hydrodynamic loads can be notably (1.5 times) higher than the quasistationary loads established at large times. The horizontal load on a submerged obstacle is identical in order of magnitude to the total dynamic-momentum flux of the jet of the lower fluid layer and depends greatly on the degree of flow blocking by the obstacle. The visualization of fluid currents performed in the work provides information on the mixing dynamics at the gravity-current head and the interaction pattern of the gravity current with the obstacle.

This work was supported by the Russian Foundation for Basic Research (Grant No. 04-01-00040) and Integration Project No. 3.13.1 of the Siberian Division of the Russian Academy of Sciences

REFERENCES

1. E. J. Hopfinger, "Snow avalanche motion and related phenomena," *Annu. Rev. Fluid Mech.*, **15**, 47–76 (1983
2. J. E. Simpson, *Gravity Currents: In the Environment and the Laboratory*, Cambridge Univ. Press, Cambridge (1997).
3. E. V. Ermanyuk and N. V. Gavrilov, "Interaction of an internal gravity current with a submerged circular cylinder," *J. Appl. Mech. Tech. Phys.*, **46**, No. 2, 216–223 (2005).
4. V. I. Bukreev and N. V. Gavrilov, "Perturbations ahead of a wing moving in a stratified fluid," *J. Appl. Mech. Tech. Phys.*, No. 2, 257–359 (1990).
5. T. B. Benjamin, "Gravity currents and related phenomena," *J. Fluid Mech.*, **31**, Part 2, 209–248 (1968).

6. V. I. Bukreev and A. V. Gusev, "Motion of a sphere in a fluid due to gravity," *J. Appl. Mech. Tech. Phys.*, **37**, No. 4, 494–501 (1996).
7. D. G. Karamanev, C. Chavarie, and R. C. Mayer, "Dynamics of free rise of a light solid sphere in fluid," *AIChE J.*, **42**, No. 6, 1789–1792 (1996).
8. L. P. Thomas, S. B. Dalziel, and B. M. Marino, "The structure of the head of an inertial gravity current determined by particle-tracking velocimetry," *Exp. Fluids*, **34**, 708–716 (2003).
9. J. O. Shin, S. B. Dalziel, and P. F. Dalziel," Gravity currents produced by lock exchange," *J. Fluid Mech.*, **521**, 1–34 (2004).
10. Ya. I. Voitkunskii, Yu. I. Faddeev, and K. K. Fedyaevskii, *Hydromechanics* [in Russian], Sudostroenie, Leningrad (1982).
11. J. S. Turner, *Buoyancy Effects in Fluids*, Cambridge, New York (1973).
12. M. I. Gurevich, *Theory of Ideal Fluid Jets* [in Russian], Nauka, Moscow (1979).
13. G. F. Lane-Serff, L. M. Beal, and T. D. Hadfield, "Gravity current flow over obstacles," *J. Fluid Mech.*, **292**, 39–53 (1995).